

Published in final edited form as:

*Curr Biol.* 2012 September 11; 22(17): 1601–1608. doi:10.1016/j.cub.2012.06.042.

## Contributions of turgor pressure, the contractile ring, and septum assembly on forces in cytokinesis in fission yeast

Stephen A. Proctor<sup>1, #</sup>, Nicolas Minc<sup>1, 2, #</sup>, Arezki Boudaoud<sup>3</sup>, and Fred Chang<sup>1, \*</sup>

<sup>1</sup>Department of Microbiology and Immunology, Columbia University College of Physicians and Surgeons, 701W 168<sup>th</sup> Street, New York, NY 10032, U.S.A.

<sup>2</sup>Institut Curie, UMR 144 CNRS/IC, 26 rue d'Ulm, 75248 Paris Cedex 05, France

<sup>3</sup>Laboratoire de Reproduction et Développement des Plantes, INRA, CNRS, ENS, Université de Lyon, 46 Allée d'Italie, 69364 Lyon Cedex 07, France

### Abstract

A paradigm of cytokinesis in animal cells is that the actomyosin contractile ring provides the primary force to divide the cell [1]. In the fission yeast *Schizosaccharomyces pombe*, cytokinesis also involves a conserved cytokinetic ring, which has been generally assumed to provide the force for cleavage [2–4] (see also [5]). However, in contrast to animal cells, cytokinesis in yeast cells also requires the assembly of a cell wall septum [6], which grows centripetally inwards as the ring closes. Fission yeast, like other walled cells, also possess high (MPa) turgor pressure [7–9]. Here, we show that turgor pressure is an important factor in the mechanics of cytokinesis. Decreasing effective turgor pressure leads to an increase in cleavage rate, suggesting that the inward force generated by the division apparatus opposes turgor pressure. The contractile ring, which is predicted to only provide a tiny fraction of the mechanical stress required to overcome turgor, is largely dispensable for ingression; once septation has started, cleavage can continue in the absence of the contractile ring. Scaling arguments and modeling suggest that the large forces for cytokinesis are not produced by the contractile ring, but are driven by the assembly of cell wall polymers in the growing septum.

## RESULTS and DISCUSSION

### Turgor pressure affects the rate of cleavage

Here, we consider the forces involved in fission yeast cytokinesis. We viewed the cylindrical *S. pombe* cell as an entity composed of a cytoplasmic fluid with a high internal turgor pressure,  $P_0$ , encased by a semi-permeable plasma membrane and an elastic cell wall [7] (Figure 1A). These mechanical properties resemble those of other walled cells such as bacteria and plants [8, 9]. For cell division, the plasma membrane ingresses centripetally from the cell surface at the medial division site, with the extracellular cell wall just outside

© 2012 Elsevier Inc. All rights reserved.

\*To whom correspondence should be addressed: Fred Chang, 701W 168<sup>th</sup> Street, New York, NY 10032, U.S.A. Tel: 212-305-0252 Fax: 212-305-1468, fc99@columbia.edu.

#These authors contributed equally to this work

**Publisher's Disclaimer:** This is a PDF file of an unedited manuscript that has been accepted for publication. As a service to our customers we are providing this early version of the manuscript. The manuscript will undergo copyediting, typesetting, and review of the resulting proof before it is published in its final citable form. Please note that during the production process errors may be discovered which could affect the content, and all legal disclaimers that apply to the journal pertain.

### Supplementary Information.

The supplement includes a description of computational models, supplementary figures and tables, movie, and additional methods.

the plasma membrane, and the contractile ring attached to the membrane on the cytoplasmic side. In contrast to bacteria, fission yeast cells cease to grow and do not change in size or shape during this process. The cell wall septum, which is composed of  $\beta$ -1,3-glucan,  $\beta$ -1,6-glucan,  $\alpha$ -1,3-glucan and  $\alpha$ -galactomannan (but no chitin) [10, 11], grows inwards centripetally as the contractile ring closes, and has a thickness,  $w$ , of about  $0.1 \mu\text{m}$  [12]. These glucan fibrils are assembled by cell wall synthase enzymes at the plasma membrane at the leading edge of the septum [13, 14]. The actinomyosin-based cytokinetic ring is thought to provide a contractile force that pulls the plasma membrane inward (Figure 1B). The ring and the septum are both essential for cytokinesis [15–17]. For instance, in contractile ring mutants, the septum is not formed [17–19], while in cells lacking a cell wall (protoplasts), the ring forms but does not cleave the cell [6]. Internal turgor pressure associated with cell growth has been estimated to be  $0.85\text{MPa}$  in fission yeast using experiments with micro-chambers [7]; if we estimate an additional  $0.1\text{MPa}$  needed for the cell wall to yield, the total turgor pressure is estimated to be  $0.95\text{MPa}$  (which will be generally presented in the text as approximately  $1\text{MPa}$ ). This pressure (similar to that of a racing bike tire) is of a similar magnitude to pressures of  $0.5$ – $5\text{MPa}$  measured in other walled cells using a variety of approaches [8, 9]. Turgor pressure has been suggested to oppose the ingression of the plasma membrane in processes such as endocytosis [20], and has been speculated to be a factor in cytokinesis [17]. We postulate that the total mechanical stress generated by the whole division apparatus should overcome this high cytoplasmic pressure to allow inward progression [21].

To test experimentally if turgor pressure is a factor in cytokinesis, we manipulated turgor pressure by adding sorbitol to the media in a *gpd1 $\Delta$*  (glycerol-3-phosphate dehydrogenase) mutant background [7, 22]. In wildtype cells, addition of sorbitol triggers an adaptive response; sorbitol induces the expression of the *gpd1<sup>+</sup>* gene through the osmotic stress response pathway, leading to synthesis of additional intracellular glycerol to cause a compensatory increase in internal turgor pressure [23]. The use of a *gpd1 $\Delta$*  mutant allows us to assay sorbitol effects on turgor pressure more directly without many of these adaptive effects. As *gpd1 $\Delta$*  cells exhibit near normal growth rates, morphology and cell tip forces in the absence of sorbitol [7], we assume that these cells have normal levels of turgor pressure in the absence of sorbitol. We predicted that addition of sorbitol, which causes a decrease in the effective turgor pressure (pressure difference between inside and outside the cell), may cause an increase in ingression rates,  $v_S$ , in a dose-dependent manner.

To test these aspects, we added sorbitol at a range of concentrations to *gpd1 $\Delta$*  cells and assayed the rate of ring closure by imaging the contractile ring marker *rlc1*-GFP (regulatory light chain of myosin II) using time lapse microscopy. In media alone ( $0\text{M}$  sorbitol), rings closed at an average rate of  $0.123 \mu\text{m}/\text{min} \pm 0.024$  ( $n=63$ ). This rate in *gpd1 $\Delta$*  cells was slightly higher than rates seen in *gpd1<sup>+</sup>* cells ( $0.117 \mu\text{m}/\text{min} \pm 0.011$ ;  $n=19$ ). To minimize possible variations arising from environmental factors (temperature or humidity), we imaged cells in sorbitol concurrently with  $0\text{M}$  control cells on the same slide, and quantified the relative changes in ingression rate.

Strikingly, we found that low concentrations of sorbitol caused the ring to close faster; at  $0.08\text{M}$  sorbitol, cell rings closed at an average of  $0.142 \mu\text{m}/\text{min} \pm 0.025$  ( $n=58$ ), which corresponds to a 16% increase (Figure 1E). This  $0.08\text{M}$  change in sorbitol concentration,  $C_S$  corresponds to a relative reduction in osmotic pressure,  $\Delta P \approx 0.2\text{MPa}$  (20%). Increases in closure rates positively correlated with increasing dose of sorbitol in a range of concentrations from  $0.02$  to  $0.08\text{M}$  (correlation coefficient,  $R=0.80$ ) (Figure 1E). These increases in rates were all significant ( $p < 0.05$  for each sorbitol concentration tested in the range of  $0.03$ – $0.08\text{M}$ ). Kymographs showed that the closure rate for each individual cell was relatively constant throughout closure in the control and sorbitol-treated cells (Figure 1C and

D). This increase was not observed in similar experiments performed in a *gpd1*<sup>+</sup> background suggesting that this change in cleavage rate was directly due to a decrease in turgor (Figure S2).

Although sorbitol clearly increased the ingression rates, the dose response curve in the low range of sorbitol concentrations, however, did not rise with sorbitol concentration as predicted, but appeared relatively flat (Figure 1E). At higher sorbitol concentrations of above 0.1M, closure rates even decreased both in a *gpd1*<sup>-</sup> and *gpd1*<sup>+</sup> backgrounds. These results suggest that there may be additional deleterious effects of high concentrations of sorbitol on cell physiology. Sorbitol concentrations above 0.4M caused the cell to shrink [7], and inhibited ring ingression; note that the reduction of effective pressure at this concentration is approximately equivalent to 1 MPa. Even at lower sorbitol concentrations (0.02 to 0.08M), it is likely that sorbitol has some inhibitory effects on cell physiology, especially in *gpd1* cells. It is also possible that the ingression rate could be limited by other factors, such as cell wall synthesis, or by other buffering mechanisms that are independent of *gpd1*. Thus, deleterious effects of sorbitol may explain why there is not a larger increase in ring closure rates with increasing sorbitol concentrations in Figure 1E.

It has been proposed that rates of ingression may correlate with the concentration of myosin in the ring [5]. To test if increased rates of ring contraction could be due to increased concentration of myosin II in the ring, we measured the number of *rlc1*-GFP molecules, which are stoichiometric with myosin II heavy chain. Quantitative fluorescence intensity measurements showed that *rlc1*-GFP intensities at the ring were similar at 0M and 0.08M sorbitol concentrations (Figure 1F). We also noted no qualitative differences in F-actin organization in the rings by phalloidin staining (Figure S2). Thus, the effects of sorbitol may be a more direct consequence of reduced outward force from turgor pressure.

### The contractile ring may provide insufficient force for cleavage

We next considered whether the contractile ring produces enough mechanical stress to counter the large internal turgor pressure. There are approximately 5000 molecules of myosin type II heavy chains (*myo2p* and *myo2p*) in a mature contractile ring [24]. We consider how much force may be maximally generated by these myosins, when all myosins pull exactly radially inward. If we assume that each single myosin molecule can exert up to 3–4pN of force [25], this suggests that the myosins in the ring together may generate a maximum force,  $f_{car}$ , on the order of 15nN. Previous estimates led to smaller values around 1nN [21, 24]. In echinoderm embryos, contractile forces roughly of 10–15 nN have been measured [1]. We estimated the inward equivalent stress generated by the ring as  $\sigma_{car} = f_{car} / (2\pi w R_0)$ . If we assumed that the ring exerts a force on the membrane over the width of the septum ( $w = 0.1 \mu\text{m}$ ) [26], this yielded values for  $\sigma_{car}$  of about 10 kPa. More detailed calculations of this stress yielded smaller values around 1kPa (see description of model in Supplementary Information). Thus, we predict that the fission yeast contractile ring can contribute only 1% or less of the stress required for division.

### Cleavage in the absence of the contractile ring

These estimates led us to test whether the ring is even needed for cleavage. Previous studies have shown that the contractile ring is essential for cytokinesis. In these experiments, blocking ring assembly in early mitosis inhibited septum formation or produced a highly abnormal one [13, 19, 27]. Thus, in addition to providing contractile force, the ring could function as a template for septum formation, for targeting the septum machinery to the division site. To test more specifically the function of the ring in force generation, we disassembled the ring in cells that had already initiated septation. We followed septum ingression using a functional GFP-*bgs4* ( $\beta$ -1,3 glucan synthase subunit) fusion, which marks

the leading edge of the septum even in the absence of actin [28]. Treatment of cells with 200 $\mu$ M Latrunculin A (LatA) causes complete inhibition of all detectable F-actin structures in the cell, as shown previously [14, 29]. We confirmed this actin inhibition for our experimental set up and strain (Figure 2A and Supplementary Figure 1).

Interestingly, in a significant fraction of these LatA-treated cells, septa continued to ingress and close (in 13 cells, n=40; Figure 2B,C), as judged by the juxtaposition of the ingressing plasma membranes. In other cases the septum promptly ceased growing. In a small subset of cases, the septa grew in a deviated manner. We found that successful septation in LatA depended on how far a septum had progressed at the time of LatA addition (Figure 2C); in general, cells that had septated more than 50% continued to ingress and appear to complete septation, while those that had only septated 50% or less ceased to ingress and exhibit cytokinesis failure or arrest. Thus, F-actin is not essential for the later stages of ingression.

Not surprisingly, septa in LatA-treated cells ingressed more slowly than septa in untreated cells (63% slower, n=6 and 8 for control and LatA-treated cells respectively, Figure 2D). F-actin has multiple functions in the septation process, not only in the actin ring, but also in endocytosis, recycling, and exocytosis, and thus these reduced rates of septum ingression could be indirect, for instance, stemming from defects in trafficking of the membrane-bound cell wall synthases. Consistent with this, in LatA-treated cells, GFP-bgs4 signal appeared in a broader distribution around the septum as compared to untreated cells, consistent with defects in endocytosis [28]. Another possibility is that the contractile ring contributes directly to optimize the rate of septum formation below.

We also tested the contribution of other contractile ring proteins to ingression. Similar to the LatA protocol, we shifted cells with temperature-sensitive mutant alleles to restrictive temperature, and monitored their ability to ingress after septation initiation. *cdc12-112* (formin) and *myo2-E1* (myosin II) mutants showed continued septation in the majority of cases (Figure 2E, F), although the rate of ingression was slower (Figure S2). One caveat of this experiment is that these temperature sensitive mutant alleles may not represent a complete loss of function, and thus do not have as a severe defect as LatA-treated cells. These data indicate that elements of the actin-myosin ring can be dispensable for later parts of cytokinesis.

### Septum assembly may drive cleavage

We next asked whether cell wall assembly could instead generate the force to override high turgor pressure. Septum assembly involves in part the polymerization of  $\beta$ -1,3 glucan polysaccharide fibrils just outside of the plasma membrane, catalyzed by multiprotein complexes of  $\beta$ -glucan synthase (encoded by the *bgs* genes), which are embedded in the plasma membrane at the division site [15, 16, 30]. Bgs1 is required for the assembly of linear (1,3) $\beta$ -D-glucans in the primary septum, which appears to guide septum formation [30]. Mutants in these *bgs* genes are defective in different aspects of septum synthesis [15, 16, 28]. To probe the effect of glucan synthesis, we examined a weak temperature sensitive allele of *bgs1* (*cps1-191*), a previously characterized mutant allele whose precise defect is not known [15, 30]. We found that these mutant cells exhibited defects in septum ingression, as measured by time-lapse microscopy. In 47% of cases, a shift to restrictive temperature after septation initiation led to failed septation (n=19), and in the subset of cells that completed septation, the rate of ingression was decreased by 34% (Figure 3A,B). Thus, cell wall synthesis contributes to ingression.

Fluorescence intensity measurements suggest that there are approximately 3000–4000 bgs1 and bgs4 molecules at the septum at the time of initial ingression (Figure 3C, D). Sorbitol treatment did not alter the number of these proteins (Figure 3E). As septation proceeds, the

signal of GFP-bgs4 at the ingressing edge of the septum gradually increased in intensity by about 40% at the end of ingression (Figure 3F; n=8). If we assume that each bgs enzyme is polymerizing a  $\beta$ -glucan fibril, these measurements suggest that there are roughly 4000  $\beta$ -glucan fibrils polymerizing at a given time at the leading edge of the septum.

We considered if the forces produced by cell wall growth are sufficient to oppose turgor pressure. As proposed in other systems [17], we used a simple ratchet-like model for septum fibril polymerization, in which the polymerization of fibrils at the plasma membrane provides a pushing force into the cytoplasm (Figure 3G). This model assumes that the rate of septum growth,  $v_s$ , is dictated by the balance between the chemical energy gained during bond addition in the polysaccharide sugar and the opposing work of turgor on the bgs protein on the other side of the membrane. The enzymatic formation of a new glycosidic bond in the polysaccharide chain releases an energy  $\Delta G_b = 2.3 \cdot 10^{-20}$  J (14 kJ/mol), and yields the lengthening of the sugar chain by  $\delta = 0.5$  nm [31]. This energy transformed into mechanical work would generate a maximum polymerization force  $F_p = \Delta G_b / \delta$ , around 45 pN for a single growing fiber. Electron micrographs of growing cell walls [32] reveal fibrils (or bundles of fibrils) with diameters around 2 nm bundled in larger stacks made of tens of fibrils that reach a length of 2–500 nm. Estimations of single fibers flexural rigidity yields a critical buckling length of about 50–100 nm and up to 10–100  $\mu$ m for stacks of fibrils (See supplementary material). These estimates suggest that the polymerization pushing force is not limited by fibers buckling. This force is exerted on the surface  $S_{bgs}$  of the  $\beta$ -glucan synthase in the membrane, thus corresponding to a polymerization pressure  $P_p = F_p / S_{bgs}$ . If we assume a 5 nm diameter for a single bgs enzyme, this yields an estimate for the polymerization pressure of a single fibril on the bgs protein to be around 2.2 MPa. We note that thermal fluctuations of the  $\beta$ -glucan synthase even under cytoplasmic turgor pressure are expected to be ample enough to allow ratchet-like monomer insertion (See supplementary material). Thus, even if chemical energy is only partially transformed to mechanical energy, this estimate shows that the polymerization of glucan fibrils is capable of exerting a local pressure on the membrane that is on the same order of magnitude as the 1 MPa turgor pressure. The stability of the polymerized fibrils and the stiffness of the meshwork then allow the ingression of the septum to progress.

We tested if this model is consistent with our experimental results on the effects of sorbitol on rates of ingression (Figure 1E). The basic assumption of this simple ratchetlike model is that the rate of a single wall fibril polymerization,  $v_p$  is given by an Arrhenius law associated with the energy  $\Delta F$  available to the new monomer:

$$v_p = u \cdot \exp\left(\frac{\Delta F}{kT}\right), \quad (\text{eq 2})$$

with  $u$  the supply rate of monomer per fibril and  $k$  the Boltzmann's constant. When polymerizing against a pressure  $P$ , the available energy is reduced and given by:

$$\Delta F = \Delta G_b - P \delta S_{bgs} \quad (\text{eq 3})$$

If we assume that the global septum ingression rate,  $v_s$  is proportional to  $v_p$ , then Eq. 2 and 3 yield a pressure-velocity relationship that describes the dependency of the septum rate on pressure, on the form of:

$$v_s(P_0 - \Delta P) = v_s(P_0) \exp\left(\frac{\Delta P}{Q}\right), \quad (\text{eq 4})$$

where  $P_0$  is the normal turgor pressure,  $\Delta P$  the pressure reduction (induced by treatment with sorbitol in the experiments) and  $Q = kT/\delta S_{bgs}$ , a critical pressure. We estimate  $Q$  to be on the order of 0.5MPa using the same values as above. When compared with the data on increasing closure rates (Figure 1E), this theoretical trend begins to overshoot experimental behavior at relatively higher sorbitol concentration ( $> 0.03M$  typically), possibly because of negative effects of sorbitol on cell physiology discussed above (Figure S2). Yet, the orders of magnitudes inferred from this model can reflect the experimental behavior. Thus, these simple scaling arguments and model can predict the observed increase in the septum velocity when pressure is decreased (Figure 1E), and provides a simple rationale for how general septum ingression rate and mechanics are linked in this system.

In summary, we elucidate some of the forces responsible for cytokinesis in fission yeast. Our sorbitol experiments suggest that turgor pressure is relevant in cytokinesis, and indicate that large mechanical stress are required to counter turgor pressure for ingression of the cleavage furrow. However, we do not rule out that there may be compensatory mechanisms that lessen the effects of turgor pressure during ingression, such as local exocytosis or “pressure” valves. High turgor pressures are also present in other walled cells, and so it is likely that similar considerations will be relevant to other cell types such as bacteria [33]. In higher plants, the initial formation of the cell wall septum inside the cell may provide a way to largely avoid this issue. Animal cells possess much lower hydrostatic pressures (e.g. 150Pa in HeLa cells, about 1000-fold less) [34], but also have significant issues during division with coordinating cortical tension with internal pressures [35].

Our results challenge previous assumptions that the contractile ring is the primary force generator for ingression in fission yeast. One surprising finding is the observation that cytokinesis continues in the absence of the contractile ring. This finding is supported by studies showing, for instance, that a *S. pombe* mutant predicted to have decreased myosin activity in the ring, ingresses at normal rates, while cells expressing two-fold more myosin II have slightly decreased rates [36]. If the ring does not provide the primary force, then what is the ring for? One important function of the ring is likely to be in the localization and organization of the septum machinery, in part by targeting delivery of the glucan synthases via membrane trafficking. Also, the ring may function as a guide in the process of septum closure. The small amount of tension in the ring may be enough to keep the edges of the ingressing septum even and in the same plane perpendicular to the cell surface. In budding yeast, mutants lacking myosin II are able to septate, but the septa are often highly disorganized [17]. Our light microscopy images show occasional examples of “crooked septa” in LatA-treated cells. The contractile ring also appears to be dispensable in certain circumstances in other cell types. In *C. elegans*, actin inhibition during the last portion of cleavage also does not halt cleavage ingression [37]. In *Dictyostelium*, cytokinesis in mutants lacking myosin II has suggested models of membrane mechanics for furrow formation [38]. In budding yeast, the motor domain of myosin is not required for cytokinesis [39]. Thus, in general, our studies add to a growing appreciation that mechanical elements in addition to the contractile ring contribute to the mechanics of cytokinesis.

Instead of a contractile ring-based mechanism, our study supports a view that cell wall synthesis provides the primary force for septum ingression. We propose that assembly of glucan fibrils provides large pushing forces against the plasma membrane through a ratchet-like mechanism, similar to ones proposed for microtubules and actin [17]. This mechanism, which would locally generate 100-fold more force than myosin contraction, may be sufficient to oppose turgor pressure. Other cross-talk between turgor and septum growth, such as lateral compression of the septum may also help ingression [40]. Actin appears to modulate the rate of ingression, possibly through indirect effects on membrane trafficking, for instance on the delivery and recycling of the glucan synthase membrane proteins. In

addition, we speculate that the ring could promote cell wall growth in this ratchet mechanism by providing tension in the membrane, for instance by pulling the membrane slightly away from the growing glucan fibrils, facilitating monomer addition. This might explain why perturbations of ring proteins such as formin *cdc12p* and myosin II exhibit slower cleavage rates [14, 36, 41, 42]. Eukaryotic cell wall synthases are generally organized in very large membrane protein complexes. Movement of the cell wall synthases in the plane of the membrane, driven by polymerizing glucan fibrils and/or internal cytoskeletal elements [43], may help produce a homogenous, organized network in the septum. There are hints that extra-cellular elements also contribute to cytokinesis even in animal cells [44, 45]. Further investigations into the biophysics of cell wall polymers and other extra-cellular elements will provide important insights into cell division mechanisms.

## Materials and Methods

### Measurement of cytokinesis rates

*S pombe* strains used are listed in Supplementary Table 1. *S. pombe* cells were generally grown at 25°C in mid-exponential phase in YE5S rich media and imaged at room temperature (23° to 26.5°) or at 36°C using an objective heater. Cells were imaged on a spinning disc confocal or widefield microscope system. Furrow ingression rates were obtained from images of cells in the medial focal planes and manually measuring the maximum distance between *rlc1*-GFP foci (or other markers) of the ring or leading edge of the septum as a function of time, and then fitting to a linear least squares regression. In the sorbitol assays, because of possible small variations such as temperature and culture conditions, we compared the rates of sorbitol-treated cells and control cells imaged on the same day, and we considered the rates normalized to the control rates ( $v/v_0$ ) taken on the same day. Ratios of rates were then averaged over all days of acquisition for a given concentration of sorbitol. For details, please see Supplementary Methods.

## Supplementary Material

Refer to Web version on PubMed Central for supplementary material.

## Acknowledgments

We thank the members of the Chang laboratory, particularly R. Basu, Z. Zhou, and I. Flor-Parra for helpful discussions and technical support, J. Moseley and J. Ribas for strains, and J. Dumais for discussion. This work was supported by NIH grants GM056836 and GM069670 (to F.C.).

## References

1. Rappaport R. Cell division: direct measurement of maximum tension exerted by furrow of echinoderm eggs. *Science*. 1967; 156:1241–1243. [PubMed: 6067406]
2. Pollard TD. Mechanics of cytokinesis in eukaryotes. *Curr Opin Cell Biol*. 2010; 22:50–56. [PubMed: 20031383]
3. Pollard TD, Wu JQ. Understanding cytokinesis: lessons from fission yeast. *Nat Rev Mol Cell Biol*. 2010; 11:149–155. [PubMed: 20094054]
4. Balasubramanian MK, Bi E, Glotzer M. Comparative analysis of cytokinesis in budding yeast, fission yeast and animal cells. *Curr Biol*. 2004; 14:R806–R818. [PubMed: 15380095]
5. Calvert ME, Wright GD, Leong FY, Chiam KH, Chen Y, Jedd G, Balasubramanian MK. Myosin concentration underlies cell size-dependent scalability of actomyosin ring constriction. *J Cell Biol*. 195:799–813. [PubMed: 22123864]
6. Jochova J, Rupes I, Streiblova E. F-actin contractile rings in protoplasts of the yeast *Schizosaccharomyces*. *Cell Biol Int Rep*. 1991; 15:607–610. [PubMed: 1934083]

7. Minc N, Boudaoud A, Chang F. Mechanical forces of fission yeast growth. *Curr Biol.* 2009; 19:1096–1101. [PubMed: 19500986]
8. Geitmann A, Ortega JK. Mechanics and modeling of plant cell growth. *Trends Plant Sci.* 2009; 14:467–478. [PubMed: 19717328]
9. Bastmeyer M, Deising HB, Bechinger C. Force exertion in fungal infection. *Annu Rev Biophys Biomol Struct.* 2002; 31:321–341. [PubMed: 11988473]
10. Perez P, Ribas JC. Cell wall analysis. *Methods.* 2004; 33:245–251. [PubMed: 15157892]
11. Humbel BM, Konomi M, Takagi T, Kamasawa N, Ishijima SA, Osumi M. In situ localization of beta-glucans in the cell wall of *Schizosaccharomyces pombe*. *Yeast.* 2001; 18:433–444. [PubMed: 11255251]
12. Osumi M, Konomi M, Sugawara T, Takagi T, Baba M. High-pressure freezing is a powerful tool for visualization of *Schizosaccharomyces pombe* cells: ultra-low temperature and low-voltage scanning electron microscopy and immunoelectron microscopy. *J Electron Microsc (Tokyo).* 2006; 55:75–88. [PubMed: 16782736]
13. Wu JQ, Kuhn JR, Kovar DR, Pollard TD. Spatial and temporal pathway for assembly and constriction of the contractile ring in fission yeast cytokinesis. *Dev Cell.* 2003; 5:723–734. [PubMed: 14602073]
14. Pelham RJ, Chang F. Actin dynamics in the contractile ring during cytokinesis in fission yeast. *Nature.* 2002; 419:82–86. [PubMed: 12214236]
15. Liu J, Wang H, McCollum D, Balasubramanian MK. Drc1p/Cps1p, a 1,3-beta-glucan synthase subunit, is essential for division septum assembly in *Schizosaccharomyces pombe*. *Genetics.* 1999; 153:1193–1203. [PubMed: 10545452]
16. Cortes JC, Ishiguro J, Duran A, Ribas JC. Localization of the (1,3)beta-D-glucan synthase catalytic subunit homologue Bgs1p/Cps1p from fission yeast suggests that it is involved in septation, polarized growth, mating, spore wall formation and spore germination. *J Cell Sci.* 2002; 115:4081–4096. [PubMed: 12356913]
17. Schmidt M, Bowers B, Varma A, Roh DH, Cabib E. In budding yeast, contraction of the actomyosin ring and formation of the primary septum at cytokinesis depend on each other. *J Cell Sci.* 2002; 115:293–302. [PubMed: 11839781]
18. Balasubramanian MK, McCollum D, Chang L, Wong KC, Naqvi NI, He X, Sazer S, Gould KL. Isolation and characterization of new fission yeast cytokinesis mutants. *Genetics.* 1998; 149:1265–1275. [PubMed: 9649519]
19. Chang F, Woollard A, Nurse P. Isolation and characterization of fission yeast mutants defective in the assembly and placement of the contractile actin ring. *J Cell Sci.* 1996; 109(Pt 1):131–142. [PubMed: 8834798]
20. Aghamohammadzadeh S, Ayscough KR. Differential requirements for actin during yeast and mammalian endocytosis. *Nat Cell Biol.* 2009; 11:1039–1042. [PubMed: 19597484]
21. Zumdieck A, Kruse K, Bringmann H, Hyman AA, Julicher F. Stress generation and filament turnover during actin ring constriction. *PLoS One.* 2007; 2:e696. [PubMed: 17684545]
22. Ohmiya R, Yamada H, Nakashima K, Aiba H, Mizuno T. Osmoregulation of fission yeast: cloning of two distinct genes encoding glycerol-3-phosphate dehydrogenase, one of which is responsible for osmotolerance for growth. *Mol Microbiol.* 1995; 18:963–973. [PubMed: 8825100]
23. Hohmann S. Osmotic stress signaling and osmoadaptation in yeasts. *Microbiol Mol Biol Rev.* 2002; 66:300–372. [PubMed: 12040128]
24. Wu JQ, Pollard TD. Counting cytokinesis proteins globally and locally in fission yeast. *Science.* 2005; 310:310–314. [PubMed: 16224022]
25. Finer JT, Simmons RM, Spudich JA. Single myosin molecule mechanics: piconewton forces and nanometre steps. *Nature.* 1994; 368:113–119. [PubMed: 8139653]
26. Kamasaki T, Osumi M, Mabuchi I. Three-dimensional arrangement of F-actin in the contractile ring of fission yeast. *J Cell Biol.* 2007; 178:765–771. [PubMed: 17724118]
27. Nurse P, Thuriaux P, Nasmyth K. Genetic control of the cell division cycle in the fission yeast *Schizosaccharomyces pombe*. *Mol Gen Genet.* 1976; 146:167–178. [PubMed: 958201]



28. Cortes JC, Carnero E, Ishiguro J, Sanchez Y, Duran A, Ribas JC. The novel fission yeast (1,3)beta-D-glucan synthase catalytic subunit Bgs4p is essential during both cytokinesis and polarized growth. *J Cell Sci.* 2005; 118:157–174. [PubMed: 15615781]
29. Chang F. Movement of a cytokinesis factor cdc12p to the site of cell division. *Curr Biol.* 1999; 9:849–852. [PubMed: 10469572]
30. Cortes JC, Konomi M, Martins IM, Munoz J, Moreno MB, Osumi M, Duran A, Ribas JC. The (1,3)beta-D-glucan synthase subunit Bgs1p is responsible for the fission yeast primary septum formation. *Mol Microbiol.* 2007; 65:201–217. [PubMed: 17581129]
31. Voet, D.; Voet, J. *Biochemistry.* 4th Edition. 2011.
32. Osumi M. The ultrastructure of yeast: cell wall structure and formation. *Micron.* 1998; 29:207–233. [PubMed: 9684351]
33. Meyer P, Gutierrez J, Pogliano K, Dworkin J. Cell wall synthesis is necessary for membrane dynamics during sporulation of *Bacillus subtilis*. *Mol Microbiol.* 2010; 76:956–970. [PubMed: 20444098]
34. Stewart MP, Helenius J, Toyoda Y, Ramanathan SP, Muller DJ, Hyman AA. Hydrostatic pressure and the actomyosin cortex drive mitotic cell rounding. *Nature.* 2011; 469:226–230. [PubMed: 21196934]
35. Sedzinski J, Biro M, Oswald A, Tinevez JY, Salbreux G, Paluch E. Polar actomyosin contractility destabilizes the position of the cytokinetic furrow. *Nature.* 2011; 476:462–466. [PubMed: 21822289]
36. Stark BC, Sladewski TE, Pollard LW, Lord M. Tropomyosin and myosin-II cellular levels promote actomyosin ring assembly in fission yeast. *Mol Biol Cell.* 2010; 21:989–1000. [PubMed: 20110347]
37. Carvalho A, Desai A, Oegema K. Structural memory in the contractile ring makes the duration of cytokinesis independent of cell size. *Cell.* 2009; 137:926–937. [PubMed: 19490897]
38. De Lozanne A, Spudich JA. Disruption of the *Dictyostelium* myosin heavy chain gene by homologous recombination. *Science.* 1987; 236:1086–1091. [PubMed: 3576222]
39. Lord M, Laves E, Pollard TD. Cytokinesis depends on the motor domains of myosin-II in fission yeast but not in budding yeast. *Mol Biol Cell.* 2005; 16:5346–5355. [PubMed: 16148042]
40. Lan H, Wolgemuth CW, Sun SX. Z-ring force and cell shape during division in rod-like bacteria. *Proc Natl Acad Sci U S A.* 2007; 104:16110–16115. [PubMed: 17913889]
41. Yonetani A, Lustig RJ, Moseley JB, Takeda T, Goode BL, Chang F. Regulation and targeting of the fission yeast formin cdc12p in cytokinesis. *Mol Biol Cell.* 2008; 19:2208–2219. [PubMed: 18305104]
42. Blanchoin L, Pollard TD, Mullins RD. Interactions of ADF/cofilin, Arp2/3 complex, capping protein and profilin in remodeling of branched actin filament networks. *Curr Biol.* 2000; 10:1273–1282. [PubMed: 11069108]
43. Utsugi T, Minemura M, Hirata A, Abe M, Watanabe D, Ohya Y. Movement of yeast 1,3-beta-glucan synthase is essential for uniform cell wall synthesis. *Genes Cells.* 2002; 7:1–9. [PubMed: 11856368]
44. Mizuguchi S, Uyama T, Kitagawa H, Nomura KH, Dejima K, Gengyo-Ando K, Mitani S, Sugahara K, Nomura K. Chondroitin proteoglycans are involved in cell division of *Caenorhabditis elegans*. *Nature.* 2003; 423:443–448. [PubMed: 12761550]
45. Xu X, Vogel BE. A secreted protein promotes cleavage furrow maturation during cytokinesis. *Curr Biol.* 2011; 21:114–119. [PubMed: 21215633]

### Highlights

- For cytokinesis, fission yeast cells cleave against a high internal turgor pressure.
- Reduction in turgor pressure causes faster cleavage.
- Assembly of the cell wall septum may provide the primary force for ingression.
- The contractile ring supplies only a minor force and is dispensable for ingression.

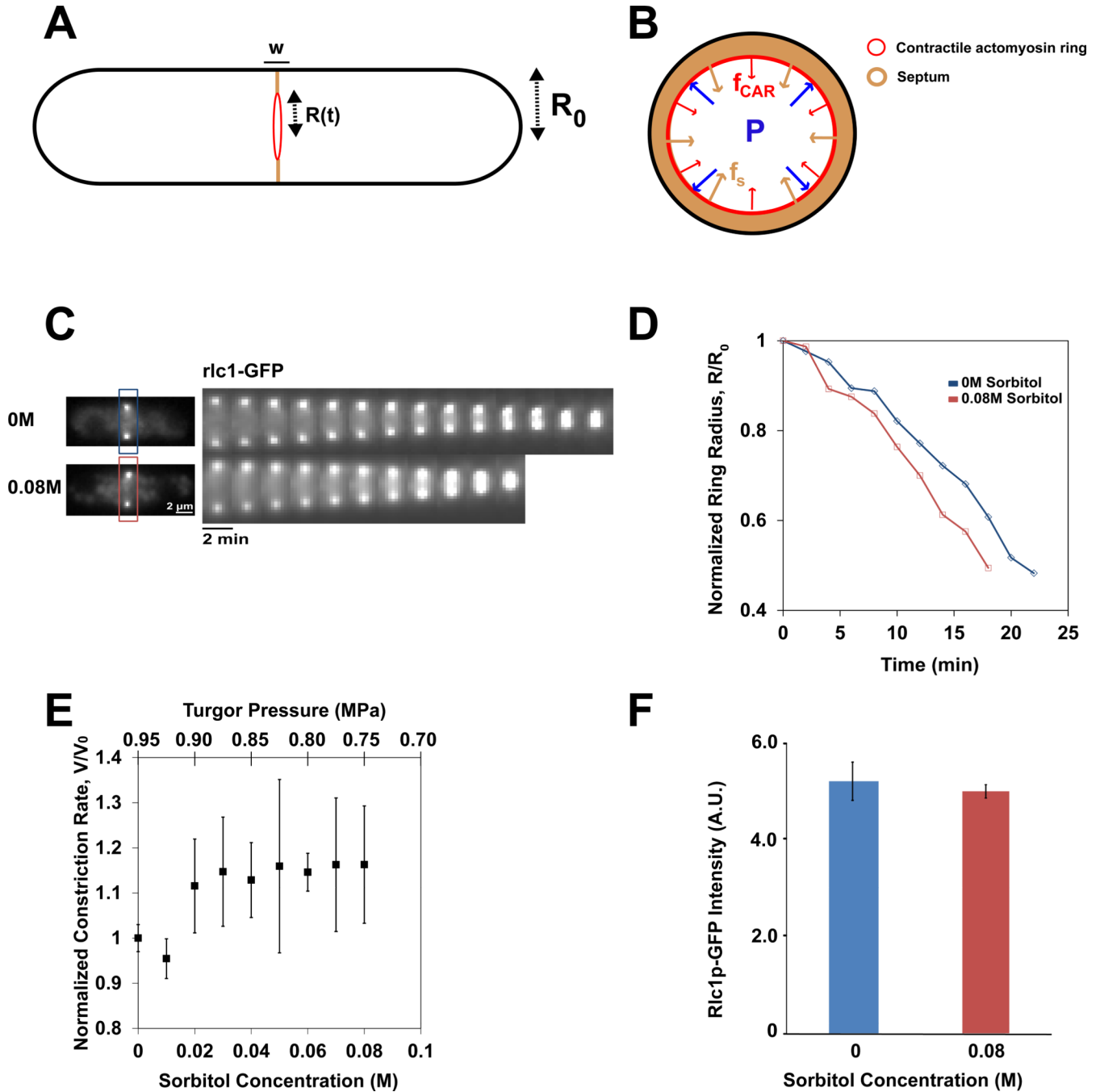


**Figure 1. Turgor pressure opposes the ingress of the cleavage furrow**

A) Schematic view of a fission yeast cell. The radius of the cell  $R_0$  is about  $2 \mu\text{m}$ , and the width  $w$  of the septum and cleavage furrow is  $0.1 \mu\text{m}$ .  $R(t)$  is the radius changing over time, at medial division plane.

B) Cross sectional view of the division site. Internal turgor pressure,  $P$ , may oppose the inward forces of ring constriction and septum cell wall growth,  $f_{\text{CAR}}$  and  $f_{\text{S}}$  respectively.

C) Time-lapse images of *gpd1Δ rlc1-GFP* cells in indicated sorbitol concentrations. Rlc1-GFP (myosin regulatory light chain) serves as a ring marker. Images were acquired at 2 min intervals at the medial focal plane.

D) Normalized ring diameter as a function of time at indicated sorbitol concentrations. Ring diameter is normalized to distance between *rlc1*-GFP foci at the beginning of respective acquisitions, at the beginning of ring closure, as imaged at medial focal plane. One line represents one cell.

E) Average relative rate of ring constriction as a function of sorbitol concentration and turgor pressure. Turgor values are computed using  $P = P_0 - \Delta P$ , with  $P_0 = 0.95 \text{ MPa}$  and  $\Delta P = 2.375 * C_s$ , with  $C_s$  in M and P in MPa. Rates were normalized to WT data taken on the same day. Error bars represent  $\pm 0.5 \text{ STD}$ . (n = 4, 5, 19, 10, 37, 11, 12, 58 cells for concentrations 0.01 M through 0.08 M respectively).

F) Average *rlc1*-GFP fluorescence in the ring of *gpd1* $\Delta$  cells at indicated sorbitol concentrations. Error bars represent  $\pm \text{STD}$ . (n=18 and 10 for 0 M and 0.08 M sorbitol concentrations respectively.)

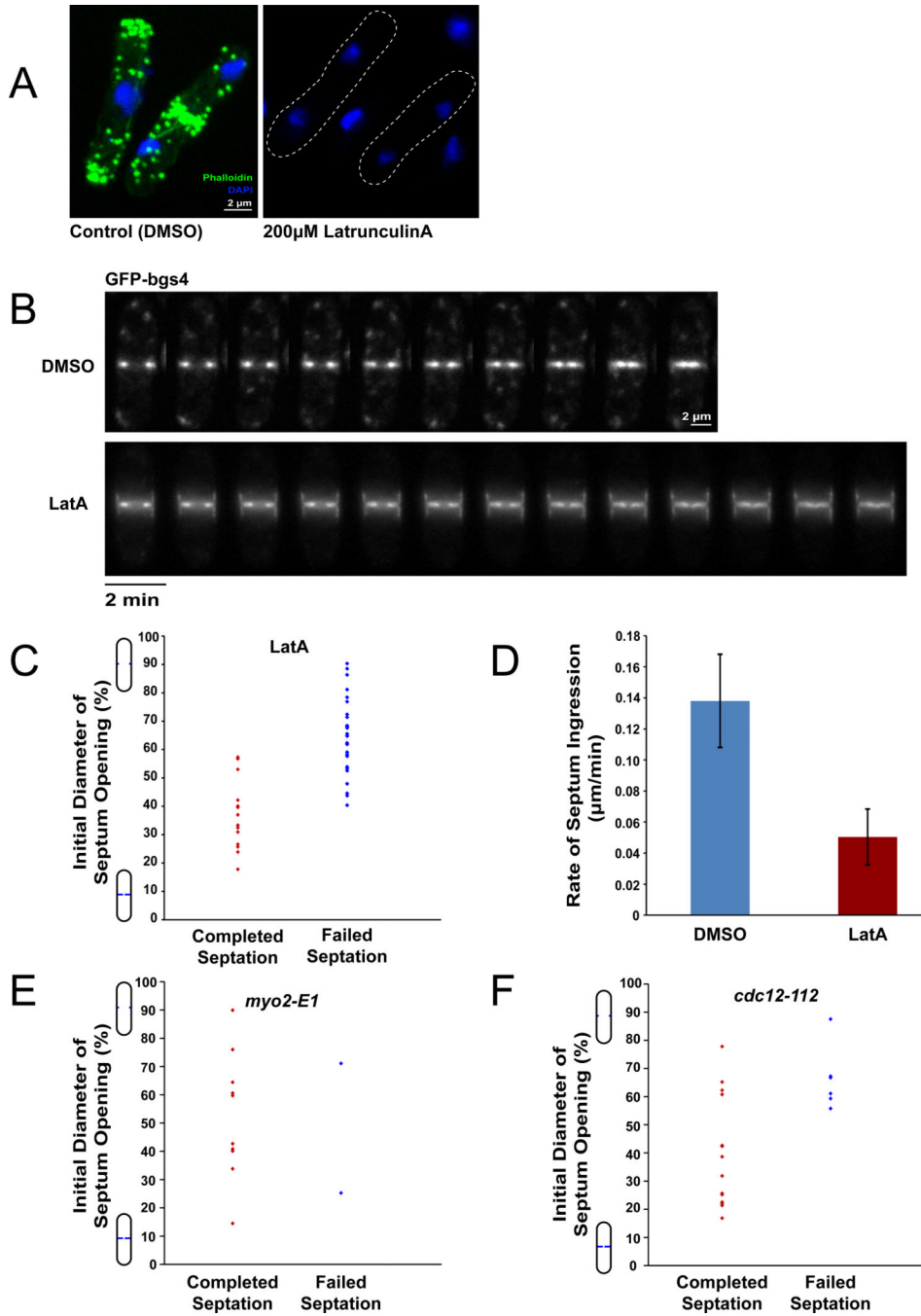


**Figure 2. Cleavage furrow ingression in the absence of the contractile ring**

A) WT cells were treated with indicated concentrations of LatA for 5 min and subsequently fixed and stained with Alexa Fluor 488-Phalloidin (F-actin) and DAPI (DNA). Maximum intensity projection confocal images are shown. No cells treated with LatA exhibited any detectable F-actin ring (or other F-actin structures).

B) Time-lapse images of WT cells treated with indicated concentrations of LatA. GFP-bgs4 expressed from its native promoter is used to mark the septum. Images were acquired at 2 min intervals at the medial focal plane. Note that the septum continues to ingress in the LatA-treated cells. See also Supplementary Movie 1.

C) The completion of septation in Lat A treated cells is dependent on the how far the septum has ingressed at time of Lat A addition. WT cells expressing GFP-bgs4 were treated with 200  $\mu$ M LatA for 5 min, then imaged at the medial focal plane for approximately 40 minutes. The completion of septation (as determined by apparent closure of the septum on these images) is plotted relative to the initial normalized distance between septa at the start of acquisition. (n=15 and n=30 for cells that completed septation and failed septation respectively).

D) Rates of septation in WT cells treated with indicated concentrations of Lat A. Error bars represent  $\pm$  STD. (n=6 and n=8 for 0  $\mu$ M and 200  $\mu$ M, respectively).

E) Septum ingression in *myo2-E1* (myosin II heavy chain) mutant cells. Cells expressing GFP-bgs4 were shifted from 25°C to 36°C and imaged for septum ingression, similar to (C). (n= 12 cells).

F) Septum ingression in *cdc12-112* (formin) mutant cells. Similar to (E). (n= 20 cells).

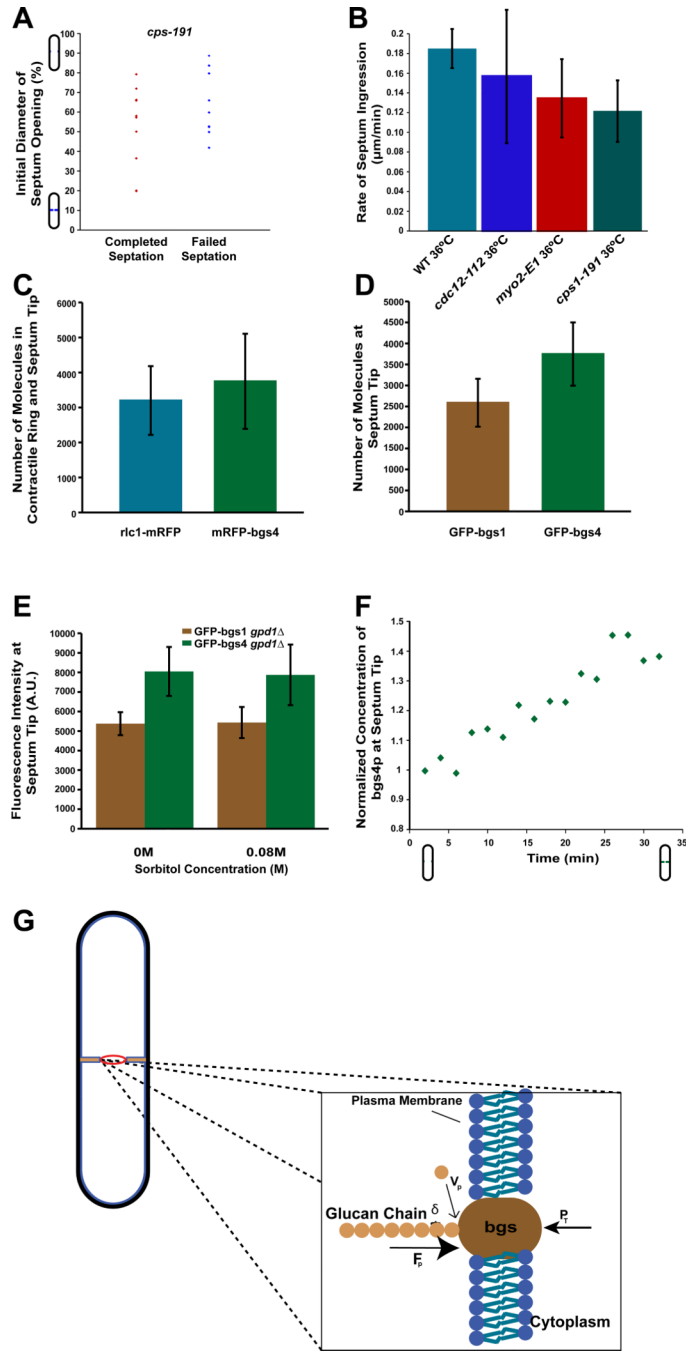


**Figure 3. Cytokinesis may be driven by cell wall assembly**

A) *cps1-191* mRFP-bgs4 cells were shifted from 25°C to the restrictive temperature of 36°C and assayed by time lapse microscopy for septum ingression. Graph plots the frequency of completed or arrested septation as a function of the initial normalized distance between septa at temperature shift. Note: t=0 when the temperature reading on the objective is 36°C. (n=19 cells)

B) Rates of furrow ingression in wildtype and mutant cells of the indicated genotype at 36°C. Only cells that appeared to complete septation were counted. Error bars represent ± STD. (n=3, 13, 10, 10 for WT, *cdc12-112*, *myo2-E1*, and *cps1-191* cells respectively)

- C) Estimating the number of bgs4p molecules at the leading edge of nascent septa (defined as septa having >85% of cell diameter between tips at medial focal plane). Fluorescence intensity measurements of mRFP-bgs4 (expressed from the *bgs4* promoter) were compared with rlc1-mRFP (myosin regulatory light chain) ring, which has previously been estimated to be a mean of 3200 molecules per ring [24]. (n=25 for rlc1-mRFP and 17 for mRFP-bgs4.)
- D) Estimating the number of bgs1p molecules. Fluorescence intensity measurements of GFP-bgs1 and GFP-bgs4 at the leading edge of nascent septa were compared, and bgs1p numbers were derived from comparison to bgs4p data in Figure 3C. (n=23 and n=22 cells for GFP-bgs1 and GFP-bgs4 cells respectively)
- E) Effect of sorbitol on bgs1p and bgs4p concentration. GFP-bgs1 and GFP-bgs4 expressing *gpd1Δ* cells were treated with indicated sorbitol concentration for > 5 min at 25°C, and fluorescence intensities were measured at the leading edge of nascent septa. Error bars represent  $\pm$  STD. (n>11 cells for each condition).
- F) Concentration of bgs4 increases during ingression. Graph shows the relative concentration of GFP-bgs4 at the tip of the ingressing septum as a function of time in a wildtype cell. Values are normalized to initial value at start of septation. Data shows representative result in a single cell, but a similar increase was seen in 8/8 cells.
- G) Model in which cytokinesis is driven by the assembly of glucan fibrils in the cell wall septum. Ratchet model of force production by polymerization of a  $\beta$ -glucan fibril at the leading edge of septum just outside the plasma membrane.  $v_p$ =rate of monomer addition,  $\delta$ =size of monomeric addition to glucan chain, P=turgor pressure applying opposing force over surface of synthase, and  $F_{pol}$ =force of polymerization generated from the free energy of monomer addition. The addition of the glucan monomer from the extracellular space is for illustrative purposes. The assembly of a glucan chain is predicted to produce MPa pressure on the bgs membrane protein, sufficient to counter turgor pressure and help drive the ingression of the plasma membrane during cytokinesis (see text).